

## Research Article

# Occurrence and Origin of H<sub>2</sub>S from Volcanic Reservoirs in Niudong Area of the Santanghu Basin, NW China

Xiangxian Ma,<sup>1,2</sup> Guodong Zheng<sup>1,2</sup>, Minliang Liang,<sup>3</sup> Dianhe Xie,<sup>4</sup> Giovanni Martinelli<sup>1,5</sup>, Wasim Sajjad,<sup>1,2</sup> Wang Xu,<sup>1,2</sup> Qiaohui Fan,<sup>1,2</sup> Liwu Li,<sup>1,2</sup> Li Du,<sup>1,2</sup> and Yidong Zhao<sup>6</sup>

<sup>1</sup>Northwest Institute of Eco-Environment and Resources, Chinese Academy of Sciences, Lanzhou 730000, China

<sup>2</sup>Key Laboratory of Petroleum Resources, Gansu Province, Lanzhou 730000, China

<sup>3</sup>Institute of Geomechanics, Key Lab of Shale Oil and Gas Geological Survey, Chinese Academy of Geological Sciences, Beijing 100081, China

<sup>4</sup>Santanghu Oil Production Plant, Tuha Oilfield Company, PetroChina, Hami 839009, China

<sup>5</sup>ARPAE Emilia Romagna, 42100 Reggio Emilia, Italy

<sup>6</sup>Beijing Synchrotron Radiation Facility, Institute of High Energy Physics, Chinese Academy of Sciences, Beijing 100049, China

Correspondence should be addressed to Guodong Zheng; [gdzhhbj@mail.iggcas.ac.cn](mailto:gdzhhbj@mail.iggcas.ac.cn)

Received 23 October 2018; Revised 8 January 2019; Accepted 30 January 2019; Published 2 June 2019

Academic Editor: Andri Stefansson

Copyright © 2019 Xiangxian Ma et al. This is an open access article distributed under the Creative Commons Attribution License, which permits unrestricted use, distribution, and reproduction in any medium, provided the original work is properly cited.

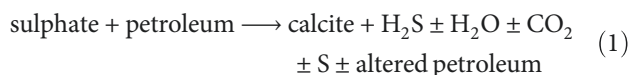
A series of samples including natural gas, formation water, and rocks were collected from volcanic rock reservoirs in the Niudong area of the Santanghu Oilfields and analyzed for their mineral and/or chemical compositions and sulfur and carbon isotopes in order to investigate the occurrence and origin of hydrogen sulfide (H<sub>2</sub>S). H<sub>2</sub>S was mostly dissolved in the formation water along with petroleum production in the study area. The  $\delta^{34}\text{S}$  values of on-well H<sub>2</sub>S samples varied in a range of 9.2‰ to 20.5‰, probably indicating thermochemical sulfate reduction (TSR) and/or thermal decomposition of organic sulfur-bearing compounds (TDS) as the genetic process for H<sub>2</sub>S. However, the chemical composition of formation waters from the Kalagang Formation (C<sub>2</sub>k) and their coefficient of desulfurization also revealed that TSR could be the main principle for H<sub>2</sub>S formation. Considering the regional geological background, especially the tectonic structures and thermal evolution features of the basin, it was concluded that H<sub>2</sub>S in the study area was dominantly produced by thermal genesis with TSR as a domain through interactions between hydrocarbons and aqueous sulfate dissolved from sulfate minerals.

## 1. Introduction

Hydrogen sulfide (H<sub>2</sub>S) is one of the most perilous constituents of natural gases and also hazardous in several aspects such as diluting the proportion of hydrocarbons in natural gas, gravely altering its economic vitality, and being extremely lethal and corrosive to equipment used for oil and gas exploration and development [1, 2]. It is significantly important to study and get a better understanding of H<sub>2</sub>S's occurrence and its origin for the reduction of health-related risks and to ensure safety, proper management of reservoirs, suitable construction facilities, and drilling-well design [3–5].

According to the literature, there are four major sources in geology for H<sub>2</sub>S from a viewpoint of genesis: (1) inorganic (volcanic) source [6], (2) bacterial sulfate reduction (BSR) [7, 8], (3) thermal decomposition of organic sulfur-bearing compounds (TDS) in oil or kerogen [5, 9], and (4) thermochemical sulfate reduction (TSR) [7, 10, 11]. Inorganic (volcanic) H<sub>2</sub>S genesis always occurs through volcanic activities and leads to a higher concentration of H<sub>2</sub>S, whose sulfur isotope is normally in a range of –1‰ to –6–7‰ V-CDT [6, 11]. BSR is the typical and important source of H<sub>2</sub>S genesis in sediments and many gas and oil reservoirs, being common in a low proportion of H<sub>2</sub>S contribution (sulfur

concentration < 3–5%). The BSR source for H<sub>2</sub>S genesis is generally considered to be active at temperatures below 80–100°C, and their sulfur isotopic ratios are mostly in a range of -5‰ and +5‰ V-CDT [7, 8, 11]. TDS normally takes place in the heating periods of organic matters and following petroleum formation. However, the H<sub>2</sub>S contribution of TDS is very low and the isotopic ratios of sulfur range from 4‰ to 12‰ V-CDT, being always related to the secondary recovery of petroleum by using steam and/or hot water [7, 11]. Finally, the most influential source for H<sub>2</sub>S production is TSR, contributing massive proportions of H<sub>2</sub>S in natural gases and presenting in numerous petroliferous basins and even in some metal sulfide deposits [5, 7, 9, 12, 13]. Their sulfur isotopic ratios are normally between 8‰ and 25‰ V-CDT [3, 14]. The TSR reactions often occur along with interactions between hydrocarbons and aqueous sulfate which is always derived from the dissolution of sulfate minerals (primarily anhydrite and also barite and celestite). Both experimental studies and field inspections have revealed that the TSR process was kinetically practicable at outset temperatures > 100°C. Suitable temperature and pH values are the important essential factors to control the reaction rate and degree of TSR [8, 15–21]. A common chemical reaction of TSR can be summarized as follows [22].



With the progression of petroleum exploitation, unconventional oil and gas resources are the vital sources for exploration. Besides clastic and carbonate rocks, volcanic rocks as reservoirs are a potential target for oil and gas exploration as well in recent times [23]. Therefore, in the current scenario, the occurrence and origin of H<sub>2</sub>S in volcanic reservoirs should be an important topic for exploration and as a supplement to the basic theory. About 100 ppm of H<sub>2</sub>S was found in several wellheads in the Niudong area, Santanghu Basin, during the oil and gas development in 2010. Since then, growing concerns on the influence of H<sub>2</sub>S on workers' health have led to the study on H<sub>2</sub>S and measures were set up to reduce the negative influences on health and equipment. However, before controlling H<sub>2</sub>S in these reservoirs, its occurrence and origin should be properly revealed. Therefore, a series of samples, including oil and gas, formation water, drilling core rocks, and on-well H<sub>2</sub>S precipitant were collected and analyzed for this purpose.

## 2. Geological Settings

The Santanghu Basin, bordered by the Junggar Basin to the west, the Tuha Basin to the south, and the Mongolia Gebi to the northeast, is a special petroleum-bearing basin with volcanic rocks as reservoirs in NW China (Figure 1(a)). The basin in an area of  $2.3 \times 10^4 \text{ km}^2$  and with accumulative petroleum reserves of more than  $3 \times 10^8$  tons has been discovered at present. Since the initial formation in the Silurian period, this basin has experienced several tectonic movements, inducing well-developed regional faults and strongly

weathered local rocks [23–25]. Volcanic eruptions frequently occurred in and around the basin during the late Palaeozoic era which probably produced some fracture channels by faulting. However, the process of volcanism was extremely intensive during the Middle Permian period. A basalt layer in a thickness of 200–600 m was developed in several parts of the basin, mainly due to crustal thinning, lithospheric subsidence, and asthenosphere upwelling [25]. The present tectonic units of the Santanghu Basin can be divided into the northern thrust uplift zone, central depression zone, and southern thrusting nappe zone. The Niudong area belongs to the central depression in the front edge of the Tiaoshan uplift and pitches the Malang depression in the northwest-southeast direction with an area of 260 km<sup>2</sup>.

The Carboniferous sequences in the study area can be classified into five formations (from bottom to top, Figure 1(b)): the Donggulubasitao Formation (C<sub>1d</sub>), Jiangbasitao Formation (C<sub>1j</sub>), Bashan Formation (C<sub>2b</sub>), Harjiawu Formation (C<sub>2h</sub>), and Kalagang Formation (C<sub>2k</sub>). The Kalagang Formation is primarily composed of fundamental intermediate volcanic lava that is incorporated within basalt, andesite, and transitional rock types [24]. Beneath the Kalagang Formation is the Haerjiawu Formation which contains hydrocarbon source rocks. Hydrocarbons from these source rocks migrated vertically into the weathered volcanic crust through faults. Reservoirs developed oil wells in the areas where there were abundant faults, and the hydrocarbons are distributed mainly in the weathered volcanic crust near the faults. The volcanic rocks of the Haerjiawu Formation alternate with source rocks. Hydrocarbons were generated from these source rocks, migrated into the weathered volcanic crust directly or through the faults, and then accumulated to construct the petroleum reservoir in the study area [23].

The maximum burial depth of the Kalagang Formation reached 1637 m in the study area, and the present strata temperature is about 55°C [26]. Since the Santanghu Basin is just located at the junction of several major tectonic belts such as the Tianshan and Altai Mountains tectonic zones, the geothermal conditions should be changed in geological evolution history. The ancient geothermal gradient could be higher than that at present [27]. The geothermal history of the study area indicates the Middle Permian magmatism which caused locally thermal anomalies, and both the Late Indosinian movement (Late Triassic and Early Jurassic period) and Late Yanshan movement (Late Jurassic period) contributed to the increase of ancient geothermal gradients in the basin and led to the maturation of organic matters in the source rocks [26]. The temperature in oil and gas reservoirs of the Kalagang Formation (C<sub>2k</sub>) reached more than 110°C during the Permian-Triassic period [26, 27].

## 3. Samples and Analysis

**3.1. Sample Collection.** Seventeen rock samples were selected from drilling cores of the Niudong area for the present study on geochemical and mineralogical characteristics of the volcanic rocks (Table 1). All the cored samples were rocks in the reservoir of Kalagang formation (C<sub>2k</sub>), including 9 basalts, 4 andesites, 2 volcanic breccia, and 2 tuff samples.

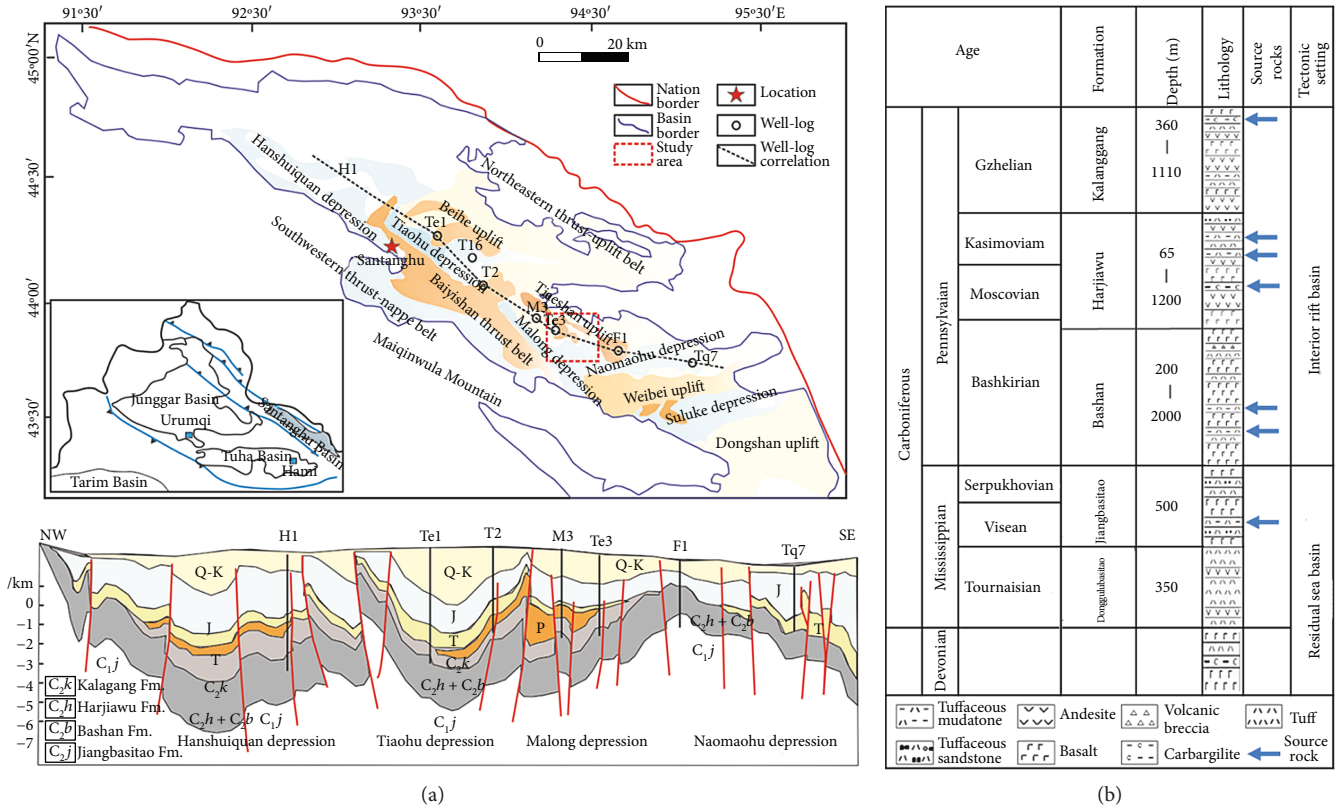


FIGURE 1: (a) Location of the study area, structure units, and section map of the Santanghu Basin. (b) Lithological column and sedimentary evolution of the Carboniferous (modified after Song et al. [24]).

TABLE 1: General property of study samples from the Kalagang Formation in the Santanghu Basin.

Sample no.	Depth (m)	Description
NDYX-01	1401.59-1401.80	Dark grey basalt
NDYX-02	1402.25-1402.39	Dark grey basalt with oil infected
NDYX-03	1403.38-1403.51	Tauro fluorescence basalt
NDYX-04	1410.81-1411.07	Tauro fluorescence basalt
NDYX-05	1416.44-1416.59	Purple basalt
NDYX-06	1420.84-1420.94	Brown basalt with oil infected
NDYX-07	1423.48-1423.62	Greyish-green breccia
NDYX-08	1429.38-1429.61	Purple oil spot andesite
NDYX-09	1429.61-1429.72	Purple oil spot andesite
NDYX-10	1430.05-1430.20	Purple oil spot andesite
NDYX-11	1433.82-1433.91	Taupe oil spot basalt
NDYX-12	1437.36-1437.51	Purple oil spot andesite
NDYX-13	1439.38-1439.49	Greyish-green breccia
NDYX-14	1444.68-1444.85	Brown-grey fluorescent basalt
NDYX-15	1447.23-1447.37	Brown-grey fluorescent basalt
NDYX-16	1508.63-1508.75	Taupe tuff
NDYX-17	1509.48-1509.56	Taupe tuff

The basalts were characterized by greyish-green and brownness and contained oil spots, air holes, and cracks. The andesites contained few and small purple oil spots and holes. The volcanic breccia and tuff were pyroclastic rocks with

TABLE 2: General properties of fillings in the crack of core samples obtained from the Kalagang Formation in the Santanghu Basin.

Sample no.	Depth (m)	Filling feature	Core
NDCT-01	1457.56-1457.68	Taupe	Dark grey basalt
NDCT-02	1552.85-1553.00	Transparent	Greyish-green basalt
NDCT-03	1540.69-1540.93	Greyish-green	Grey-brown basalt
NDCT-04	1508.63-1508.75	White	Taupe tuff
NDCT-05	1509.48-1509.56	White vein	Taupe tuff
NDCT-06	1430.05-1430.20	Milky white	Purple andesite

greyish-green and taupe, respectively. Six samples with clear veins were selected, and the vein fillings were extracted by indoor drilling for sulfur and carbon isotope analysis (Table 2 and Figure 2). The veins were in white color and transparent, some of which were characterized in an X-type of joints.

The samples for H<sub>2</sub>S isotopes were obtained from twelve production wells and one gas gathering station. For sampling, the mixture of natural gases was introduced into a pre-prepared cadmium acetate solution (Cd (CH<sub>3</sub>COO)<sub>2</sub>·3H<sub>2</sub>O), and then the precipitant of cadmium sulfide (CdS) was collected in situ by filtration for laboratory analysis.

3.2. Analytical Methods. All the rock samples without chemical pretreatment were crushed into powder by using an agate mortar and pestle. Mineralogical measurements were carried

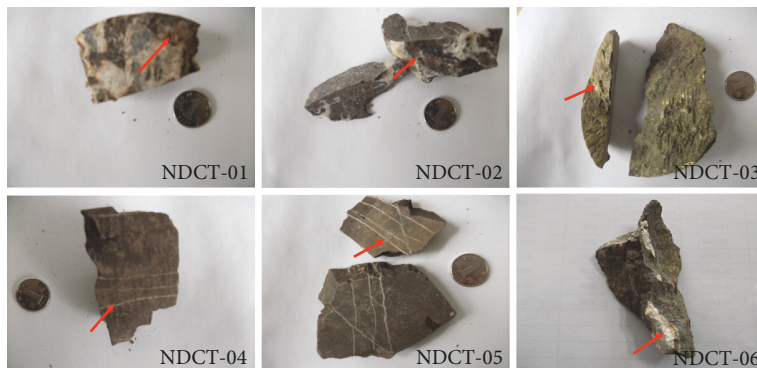


FIGURE 2: Photos showing the veins of cored samples.

out by the powder X-ray diffraction (XRD) method, using a D/Max-3B X-ray diffraction (XRD) Bruker diffractometer equipped with a graphite monochromator and operated at 40 kV and 100 mA using Cu  $K\alpha$  radiation. A small portion of finely powdered sample crushed again in a clean mortar was properly mounted on a plastic holder ( $\phi 25$  mm, depth 1 mm). Scanning of samples was performed over an interval of  $2\text{--}60^\circ$  ( $2\theta$ ) at a scanning speed of  $2^\circ/\text{min}$  for every  $0.03^\circ$  ( $2\theta$ ) step. Divergence, scattering, and receiving slits were  $0.5^\circ$ , 0.5, and 0.10 mm, respectively.

Sulfur K-edge XANES analysis of well-crushed either cored rock or drilled vein samples was performed at beamline 4B7A of the Beijing Synchrotron Radiation Facility (BSRF), Beijing. Both the beam path and samples were positioned in a vacuum to overcome the scattering of X-ray and their absorption by air when the crushed samples were exposed to the X-ray beam with an incident angle of  $45^\circ$ . The X-ray fluorescence emitted during analysis was quantified by using a solid-state detector (Si). As a reference, the spectrum of the blank filter was also measured for the comparison purpose and the absorption of sulfur was negligible [28].

The isotopic composition of sulfur (S) was analyzed by using an isotope mass spectrograph (Model MAT271) produced by Finnigan MAT Company. The mass range is 1 to 700 amu, and the mass resolution is 220 to 3000 used for gas composition and stable isotope analysis. CdS and CuO (copper oxide) obtained through precipitation were mixed in a 1:3 weight ratio into a quartz tube and rapidly heated to  $850^\circ\text{C}$  inside the reaction furnace for 30 minutes. Subsequently, the released gas was collected inside the cold trap by using liquid nitrogen for freezing the gas, and the vacuum pump was started to eliminate the impurities and pure  $\text{SO}_2$  was released. The obtained gas was introduced into the instrument for isotope analysis and the  $\delta^{34}\text{S}$  value of sulfide was ultimately obtained by using an international standard (CDT), with an accuracy of  $\pm 0.5\%$ .

Calcite presented inside the vein fillings of rock samples was extracted by using a small driller and was subjected to carbon and oxygen isotopic analysis. About 50–100 mg of calcite samples was treated with pure phosphoric acid for 4 hours at  $72^\circ\text{C}$  under a vacuumed container. The released  $\text{CO}_2$  was analyzed for carbon and oxygen isotopes by using a Finnigan MAT253 plus mass spectrometer

standardized with GBW04416. The obtained data of carbon and oxygen were reported in units/mL relative to the V-PDB standard. The precision for both  $\delta^{13}\text{C}$  and  $\delta^{18}\text{O}$  measurements was  $\pm 0.5\%$ .

The composition of formation water and the concentration of  $\text{H}_2\text{S}$  were measured by the Sangtangu Oil Production Plant of Tuha Oilfield Company. A portable hydrogen sulfide detector was used to monitor the  $\text{H}_2\text{S}$  concentration at the wellhead of Oilfield, the precision being better than 5%.

## 4. Results and Discussion

**4.1. Occurrence of  $\text{H}_2\text{S}$ .** During the first recovery of oil in the Santangu Oilfield, the  $\text{H}_2\text{S}$  content was reported in the oil-wellhead as 10–120 ppm/ $\text{m}^3$  air in 2010, and the relative content of  $\text{H}_2\text{S}$  in the dissolved air of formation water reached 0.19%. The average pressure value of reservoir strata  $C_2k$  in the study area was 10.5 MPa, of which the  $\text{H}_2\text{S}$ -bearing wells were mostly located in the area with low pressure (3–9 MPa) [29], and fractures were strongly developed in the surrounding rocks. Furthermore, the oil-wells containing  $\text{H}_2\text{S}$  more than 100 ppm were always characterized with a higher water cut (65–100%) while other oil-wells in lower  $\text{H}_2\text{S}$  concentration (<30 ppm) were assigned to a lower water cut (<60%). Thus,  $\text{H}_2\text{S}$  was mainly distributed in oil-wells with low formation pressure, high water cut, and fractures developed and mostly dissolved in formation water.

**4.2. Minerals and Sulfur Characteristics of Reservoir Rocks.** The reservoir rocks of the Santangu Oilfields are typical volcanic rocks of the Carboniferous Kalagang Formation, which are dominated by basalt, andesite, volcanic breccia, and tuff [23]. The  $\text{SiO}_2$  content of the volcanic rocks is 44% to 65%. There are a number of air holes and almond constructs in the rocks so that these rocks have relatively high porosity and proper connectivity; the porosity is 6% to 11% [23]. Weathering and leaching during the cessation of deposition should be the major controlling factor of favorable reservoirs in the Carboniferous volcanic rocks, and the secondary minerals such as clay minerals could be largely formed. The hydrolysis belt was mainly composed of mudstone and tiny volcanic grains, most of which were broken down into clay minerals [23]. The cracks or vein fillings in the



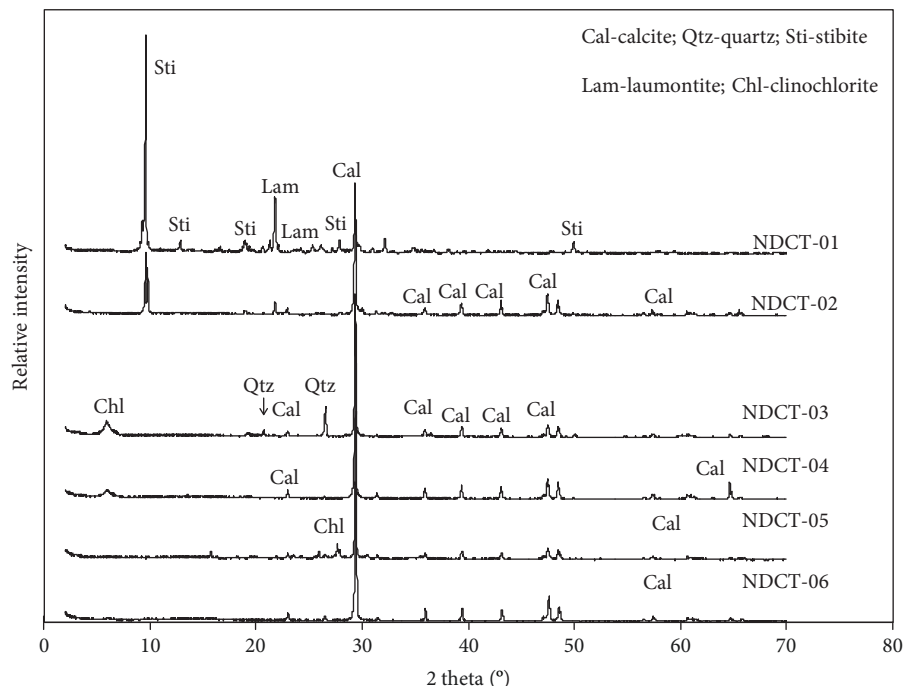


FIGURE 3: Powder X-ray diffraction patterns for the study samples.

core of volcanic rocks were widely developed and mainly consisted of volcanic zeolites, quartz, and/or calcite (Figure 3).

Sulfur species were herein referred to as the chemical status of sulfur, which was identified using XANES in this study by comparison of the obtained spectra for samples with those of selected sulfur-containing reference materials such as pyrite ( $\text{FeS}_2$ ), pyrrhotite ( $\text{FeS}$ ), calcium sulfate ( $\text{CaSO}_4$ ), and sulfur ( $\text{S}^0$ ). The impact of self-absorption associated with reference materials was investigated by using well-crushed mixtures of boron nitride in various concentrations of sulfur. The self-absorption impact was not detected in sulfur concentration  $< 0.5$  wt.% [28]. The peak positions obtained from the cored samples were mostly positioned at two series of comparable energy range to those presented in the spectra of pyrite, pyrrhotite, and calcium sulfate, signifying that the foremost sulfur species were sulfide and sulfate, respectively. The absorbing peaks presented on the left (in range of 2.470–2.474 keV) indicate the presence of  $\text{S}^{2-}$ ,  $\text{S}_2^{2-}$ , and also possibly elemental sulfur ( $\text{S}^0$ ). On the other hand, the peak presented on the right (in range of 2.481–2.484 keV) denotes  $\text{SO}_4^{2-}$  species (Figure 4). The spectra thus obtained for all samples are shown in Figure 4, in which several composite variations within numerous sulfur species are displaced based on their spectrum structures as well as the location of the peak that is signified as sulfides and/or sulfate, respectively. In this study, it was found that both the sulfate (more than 90%) and sulfide minerals widely coexisted in the reservoir rocks, which could provide an effective sulfur source for the genesis of  $\text{H}_2\text{S}$  gas within the reservoirs.

**4.3. Characteristics of Formation Water.** The chemical compositions of formation water are shown in Table 3 and Figure 5. Relatively most samples belong to the group of

$\text{Na}(\text{K})\text{-Cl}$  or  $\text{Ca-Cl}_2$  water while the existence of  $\text{Ca}(\text{Mg})\text{-SO}_4$  waters indicates possible evolutionary trends toward  $\text{SO}_4$ -enriched waters. There are no samples belonging to the  $\text{Ca}(\text{Mg})\text{-HCO}_3$  and  $\text{Na}(\text{K})\text{-HCO}_3$  groups in the study area. In particular, the  $\text{Na}^+ + \text{K}^+$  concentration of formation water in Kalagang Formation ( $\text{C}_2k$ ) was in a range of 69–1008 mg/L and the  $\text{Cl}^-$  concentration in a range of 309–1955 mg/L, respectively. The range of  $\text{Mg}^{2+}$  concentration of  $\text{C}_2k$  formation water was from 1 to 291 mg/L with an average of 56.6 mg/L. Generally, the higher the  $\text{Mg}^{2+}$  concentration, the higher would be the  $\text{H}_2\text{S}$  yields, because ion  $\text{Mg}^{2+}$  could play a catalysis role in TSR [30–32]. The range of  $\text{SO}_4^{2-}$  concentration was from 27 to 1288 mg/L. The coefficient of desulfurization ( $100 \times r \text{SO}_4^{2-}/\text{Cl}^-$ ) was in a range of 2–160 with a mean value of 30. This coefficient could be used to reflect consumption of  $\text{SO}_4^{2-}$  during TSR and the redox conditions of formation water. The low mark means reduced condition and active TSR reactions [32]. The  $\text{H}_2\text{S}$  contraction rose with a decrease in the coefficient of desulfurization (Figure 6), exhibiting that TSR really occurred in the study reservoirs. The  $\text{CO}_3^{2-}$  concentration in most water samples was low (mostly not detected), and the average of  $\text{HCO}_3^-$  was 335.8 mg/L. In addition, the concentration of  $\text{HCO}_3^-$  decreased with the process of TSR reactions, strongly indicating the dilution of additional water under TSR conditions. This kind of dilution might be lowering the concentration of  $\text{CO}_3^{2-}$  and  $\text{HCO}_3^-$  in formation waters of volcanic reservoirs.

**4.4. Sulfur Isotopes of  $\text{H}_2\text{S}$ .** The sulfur isotopes of sulfates and/or sulfides presented in the volcanic rocks from wells ND89-9 and ND89-10 are quite close to each other, being 9.2‰ and 10.3‰, respectively. The natural gases at the

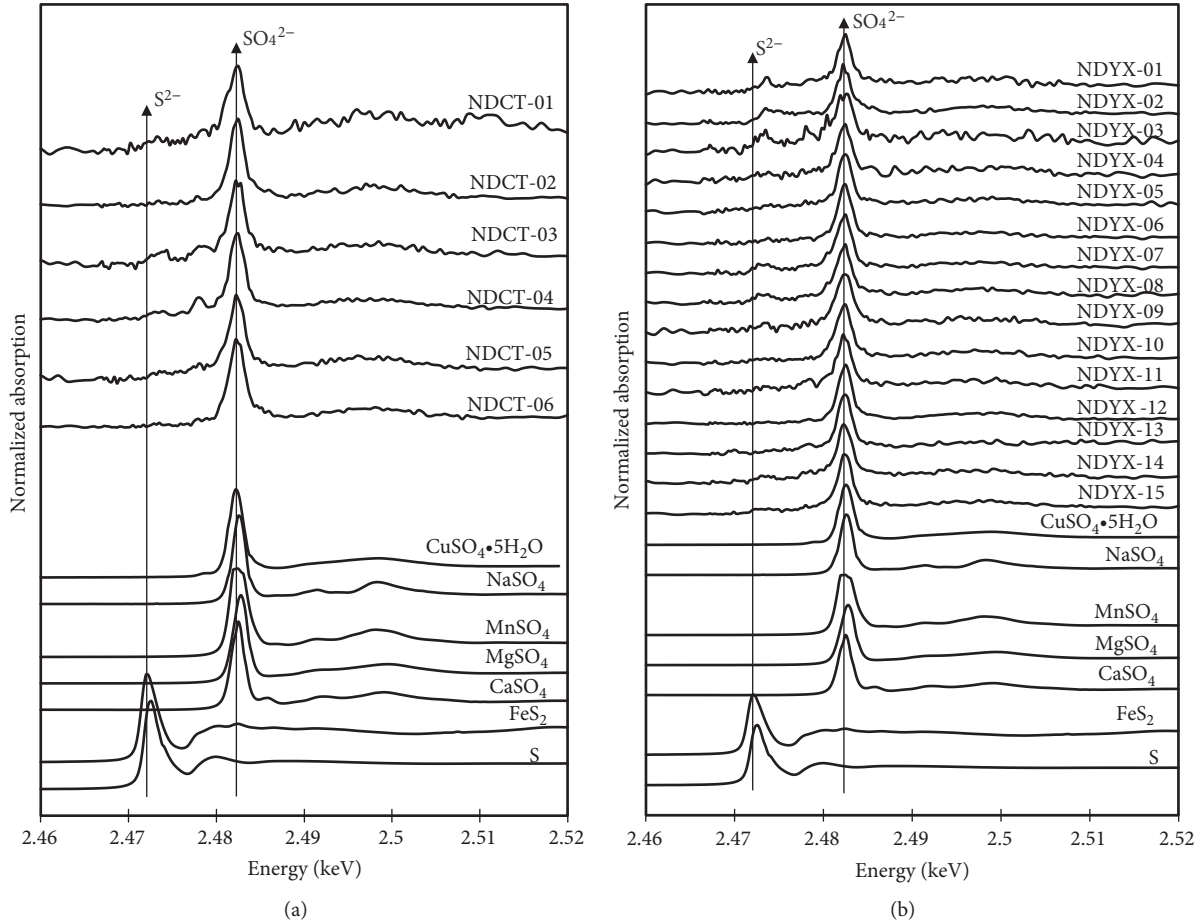


FIGURE 4: Spectra of sulfur species in the study samples. (a) Filling materials in the veins of cored rocks and (b) core samples. The absorbing peak on the left with a lower energy range corresponds to sulfides whereas the peak on the right with a higher energy range corresponds to sulfate.

TABLE 3: Hydrochemistry of the formation water from the Niudong area, Santanghu Basin.

Sample no.	Stratum	Sampling date	H <sub>2</sub> S (ppm/m <sup>3</sup> air)	K <sup>+</sup> +Na <sup>+</sup>	Ca <sup>2+</sup>	Mg <sup>2+</sup>	Cl <sup>-</sup>	mg/L			Total salinity	Type	pH
								SO <sub>4</sub> <sup>2-</sup>	HCO <sub>3</sub> <sup>-</sup>	CO <sub>3</sub> <sup>2-</sup>			
ND8-14	C <sub>2</sub> k	2008/8/7	n.d.	410	864	291	1755	920	710	268	5218	CaCl <sub>2</sub>	9.3
ND78-9	C <sub>2</sub> k	2008/8/6	115	592	545	1	1652	32	164	n.d.	2986	NaCl <sub>2</sub>	7.3
ND78-812	C <sub>2</sub> k	2010/8/7	6	371	123	10	512	283	168	n.d.	1467	NaCl	6.0
ND89-10	C <sub>2</sub> k	2010/10/8	44	647	442	24	1375	329	397	n.d.	3214	CaCl <sub>2</sub>	7.0
ND8-11	C <sub>2</sub> k	2008/8/7	35	1008	683	67	1955	434	1171	n.d.	5318	NaCl	6.5
ND89-9	C <sub>2</sub> k	2008/11/4	31	592	521	14	1544	349	123	n.d.	3143	NaCl <sub>2</sub>	6.0
ND8-111	C <sub>2</sub> k	2010/5/1	13	194	566	98	1272	47	482	n.d.	2659	CaCl <sub>2</sub>	7.0
ND89-812	C <sub>2</sub> k	2010/8/24	25	69	315	21	309	495	85	n.d.	1294	CaSO <sub>4</sub>	6.0
ND9-9	C <sub>2</sub> k	2010/3/7	50	547	384	15	1393	188	57	n.d.	2584	CaCl <sub>2</sub>	7.0
ND89-91	C <sub>2</sub> k	2010/6/5	44	869	369	15	1324	495	596	n.d.	3668	NaCl	6.0
ND 8-71	C <sub>2</sub> k	2007/12/21	120	386	396	7	1264	27	36	10	2126	CaCl <sub>2</sub>	9.0
ND8-10	C <sub>2</sub> k	2007/10/16	13	394	873	122	1475	1288	143	n.d.	4295	CaCl <sub>2</sub>	7.7
ND8-8	C <sub>2</sub> k	2008/8/7	10	537	404	51	1368	255	234	n.d.	2849	NaCl <sub>2</sub>	6.5

Note: these data were provided by the Santanghu Oil Production Plant of Tuha Oilfield Company. pH was tested at room temperature.

Niudong pumping station have undergone a series of technological operations such as separation of oil and gas, whose sulfur isotopic ratios reached 20.5‰ (Table 4). As shown in

Figure 7, the  $\delta^{34}\text{S}_{\text{V-CDT}}$  values for TSR-H<sub>2</sub>S in this study were comparable with those in the Sichuan Basin (main frequency: 8‰ to 26‰) [14], the Tarim Basin (14‰ to 19‰) [17, 33],

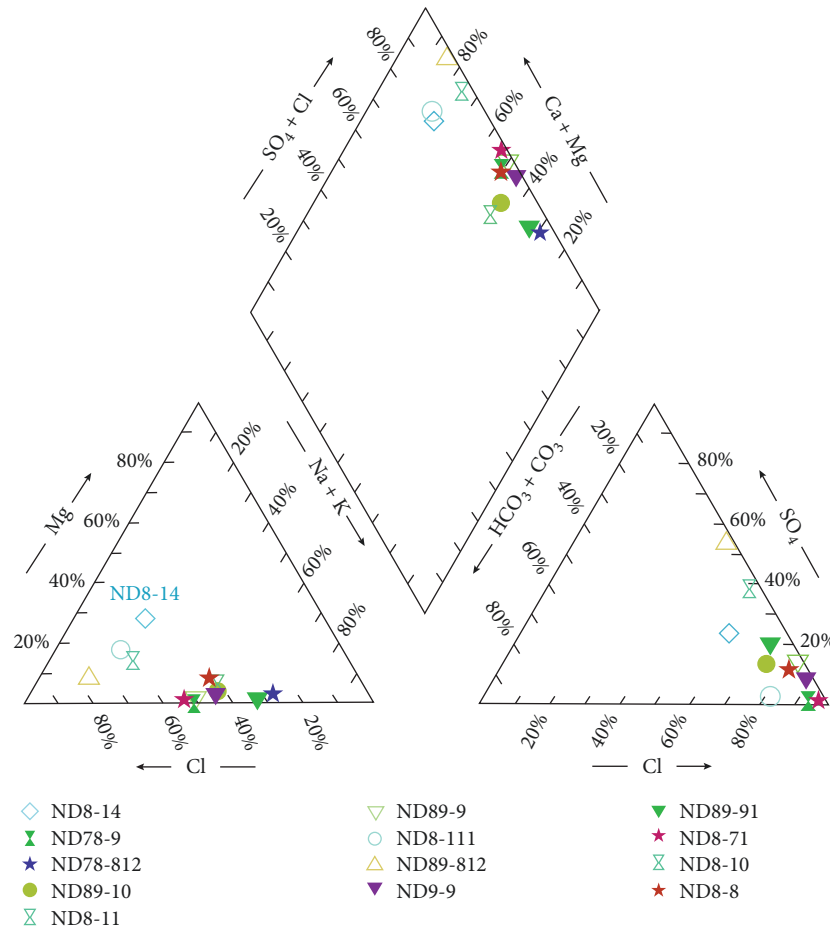


FIGURE 5: Piper diagram for ion composition of study formation waters.

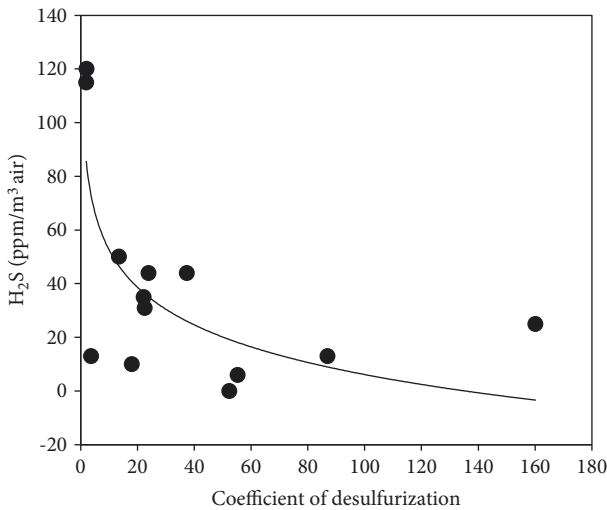


FIGURE 6: Relationship between the coefficient of desulfurization ratios and H<sub>2</sub>S concentrations of oil wells.

and the Ordos Basin (16‰ to 20‰) [14]. Such comparison may indicate that H<sub>2</sub>S presented in the oil wells of the Niudong area could probably be derived from TSR. δ<sup>34</sup>S<sub>V-CDT</sub> of TDS-H<sub>2</sub>S in crude oils is usually from 3‰ to 15‰ [5]; thus, H<sub>2</sub>S

in the Niudong area could also be due to TDS. However, there is lack of meaningful evidence for the possibility of inorganic (volcanic) origin and BSR involvement for H<sub>2</sub>S in the study area.

**4.5. Carbon Isotopes of Calcite.** The isotopic data of the calcite matrix from the Kalagang Formation exhibited a relatively wider range of carbon isotopic values between -10.7‰ and -3.3‰ V-PDB and a narrower range of oxygen isotopic values between -21.8‰ and -18.6‰ V-PDB, respectively (Table 4). These relatively negative carbon isotopic values may suggest a possible contribution of organic carbon into calcite, but the carbon and oxygen isotopic values failed on the boundary of TSR calcite [22] which was formed through TSR reactions. In addition, these carbon and oxygen isotopic values of vein calcite were also similar to those of primarily igneous carbonatite (δ<sup>13</sup>C<sub>V-PDB</sub>‰: -5.0‰ to -8.0‰, δ<sup>18</sup>O<sub>V-PDB</sub>‰: -21.7‰ to -23.7‰) [34], indicating the calcite formation with fluids from deep layers under low hydrothermal temperatures (<167°C) [35]. Therefore, calcite in the rock veins was mostly of magmatic origin and very less produced due to TSR reactions.

**4.6. Origin of H<sub>2</sub>S.** As for the low concentration of H<sub>2</sub>S in crude oils and natural gases, the BSR origin is always regarded as the first originating mechanism that may be

TABLE 4: Sulfur and carbon isotope of samples obtained from the Kalagang Formation in the Santanghu Basin.

Well or sample no.	Type	$\delta^{34}\text{S}_{\text{V-CDT}}\text{‰}$	$\delta^{13}\text{C}_{\text{V-PDB}}\text{‰}$	$\delta^{18}\text{O}_{\text{V-PDB}}\text{‰}$	Note
Gas pumping station	Gas	20.5			
ND89-9	Gas in water	9.2			
ND89-10	Gas in water	10.3			
NDCT-03	Rock		-10.7	-20.6	Calcite
NDCT-04	Rock		-5.8	-21.8	Calcite
NDCT-05	Rock		-5.7	-18.6	Calcite
NDCT-06	Rock		-3.3	-21.4	Calcite

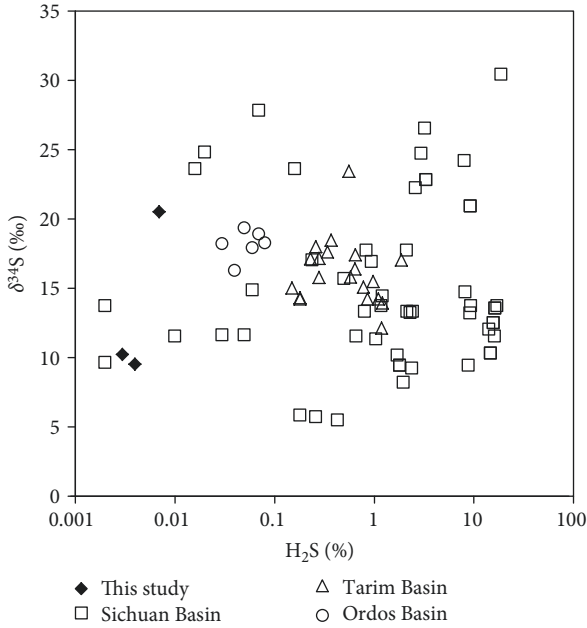


FIGURE 7: Correlation between  $\delta^{34}\text{S}$  values and  $\text{H}_2\text{S}$  contents of samples from the Santanghu Basin and other referenced TSR  $\text{H}_2\text{S}$ -bearing basins in China (data of Sichuan Basin, Tarim Basin, and Ordos Basin are from Zhu et al. [14] and Jiang et al. [22]).

caused by bacterial loadings during water injection. The sulfur isotopes of  $\text{H}_2\text{S}$  in the study area were 9.2‰ to 20.5‰, suggesting that BSR was probably not the most possible source in the Niudong Oilfield, where  $\text{H}_2\text{S}$  was found in the first recovery of oil without water injection in early oil and gas exploration. Additionally, the values of sulfur isotopes are not in favor of volcanic sources for the genesis of  $\text{H}_2\text{S}$ . Therefore, TSR and TDS should be their possible origins that were supported by the sulfur isotopic data. However, TDS usually occurred during the secondary recovery of oil under a relatively higher temperature than under the initial temperature of TSR [5], but no steam and/or hot water was utilized during the secondary recovery of heavy oils in the study reservoir and the heavy oils was typically low in sulfur content (about 0.17%). Based on these facts, either TDS should not be the origin or slightly contributed if TDS occurred. As for TSR, although gypsum and/or anhydrite in the cored rocks was not observed by naked eyes, trace sulfate and sulfide were detected by XANES. Such sulfur-bearing materials in the reservoir rocks could supply enough sulfur for TSR reactions

due to the huge volume of rocks. Secondly, the local geothermal temperature ( $>110^\circ\text{C}$ ) reached the reaction conditions for TSR during the Permian-Triassic period as for the volcanic activity [27]. Finally, some increase in  $\text{H}_2\text{S}$  concentration was observed with a decrease in desulfurization coefficient, which confirmed the occurrence of TSR. Such formed  $\text{H}_2\text{S}$  in the reservoir of volcanic rocks is easily dissolved in the formation water. On the other hand,  $\text{CO}_3^{2-}$  and  $\text{HCO}_3^-$  concentrations in most samples were relatively low, indicating that the additional water formed along with TSR may dilute the concentrations of both  $\text{CO}_3^{2-}$  and  $\text{HCO}_3^-$ . Considering all the evidences above, TSR should be the main source for  $\text{H}_2\text{S}$  in the natural gases of the Niudong Oilfield, but the TDS origin could not also be excluded.

## 5. Conclusions

The volcanic reservoir rocks of the Carboniferous Kalagang Formation are dominated by basalt and andesite, whose cracks or vein fillings in the core are mainly composed of volcanic zeolites, quartz, and/or calcite. Both sulfate (more than 90%) and sulfide minerals extensively existed in the reservoir rocks, which could provide a potential sulfur source for  $\text{H}_2\text{S}$  gas formation through TSR in the reservoirs.

$\text{H}_2\text{S}$  was distributed in the producing wells with low formation pressure and high water cut of the oil wells, which was mostly dissolved in the formation water. The sulfur isotopic data and ion compositions of formation water indicated that TSR should be the main source for  $\text{H}_2\text{S}$  genesis. The geological structures of the basin, the mineral compositions of the reservoir rocks, and the evolution characteristics of the paleogeothermal temperatures provided effective conditions for TSR reactions in the study area.

## Data Availability

The data used to support the findings of this study are included within the article.

## Conflicts of Interest

The authors declare that they have no conflicts of interest.

## Acknowledgments

This work was supported by the Natural Science Foundation of China (41572352, 41872141) and the Santanghu Oil

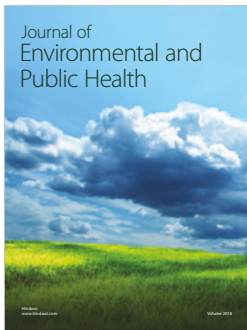
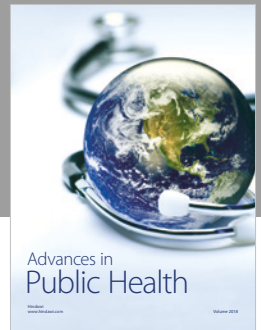


Production Factory, partially supported by the CAS “Light of West China” Program, CAS Visiting Professorship for Senior International Scientists to GM (2018VMA0007), Technology Major Project of the Ministry of Science and Technology of China (2016ZX05007001-004), and the Key Laboratory Project of Gansu Province (Grant No. 1309RTSA041). The authors are grateful to the Santanghu Oil Production Factory for the support in fieldwork and permission to use the basic geological data.

## References

- [1] R. H. Worden and P. C. Smalley, “H<sub>2</sub>S-producing reactions in deep carbonate gas reservoirs: Khuff Formation, Abu Dhabi,” *Chemical Geology*, vol. 133, no. 1-4, pp. 157–171, 1996.
- [2] G. Zhu, S. Zhang, Y. Liang, J. Dai, and J. Li, “Isotopic evidence of TSR origin for natural gas bearing high H<sub>2</sub>S contents within the Feixianguan Formation of the Northeastern Sichuan Basin, Southwestern China,” *Science in China Series D: Earth Sciences*, vol. 48, no. 11, pp. 1960–1971, 2005.
- [3] S. Zhang, G. Zhu, Y. Liang, J. Dai, H. Liang, and M. Li, “Geochemical characteristics of the Zhaolanzhuang sour gas accumulation and thermochemical sulfate reduction in the Jixian Sag of Bohai bay basin,” *Organic Geochemistry*, vol. 36, no. 12, pp. 1717–1730, 2005.
- [4] P. Mougin, V. Lamoureux-Var, A. Bariteau, and A. Y. Huc, “Thermodynamic of thermochemical sulphate reduction,” *Journal of Petroleum Science and Engineering*, vol. 58, no. 3-4, pp. 413–427, 2007.
- [5] G. Zhu, S. Zhang, H. Huang et al., “Induced H<sub>2</sub>S formation during steam injection recovery process of heavy oil from the Liaohe Basin, NE China,” *Journal of Petroleum Science and Engineering*, vol. 71, no. 1-2, pp. 30–36, 2010.
- [6] P. Allard, “The origin of water, carbon, sulfur, nitrogen and rare gases in volcanic exhalations: evidence from isotope geochemistry,” *Forecasting Volcanic Events*, H. Tazieff and J.-C. Sabroux, Eds., pp. 337–386, Elsevier, 1983.
- [7] W. L. Orr, “Changes in sulfur content and isotopic ratios of sulfur during petroleum maturation—study of big horn basin Paleozoic oils,” *AAPG Bulletin*, vol. 58, pp. 2295–2318, 1974.
- [8] H. G. Machel, “Bacterial and thermochemical sulfate reduction in diagenetic settings — old and new insights,” *Sedimentary Geology*, vol. 140, no. 1-2, pp. 143–175, 2001.
- [9] R. H. Worden, P. C. Smalley, and S. A. Barclay, “H<sub>2</sub>S and diagenetic pyrite in North Sea sandstones: due to TSR or organic sulphur compound cracking?,” *Journal of Geochemical Exploration*, vol. 78-79, pp. 487–491, 2003.
- [10] H. G. Machel, H. R. Krouse, and R. Sassen, “Products and distinguishing criteria of bacterial and thermochemical sulfate reduction,” *Applied Geochemistry*, vol. 10, no. 4, pp. 373–389, 1995.
- [11] Z. Guang-you, Z. Shui-chang, L. Ying-bo, and D. Jin-xing, “Stable sulfur isotopic composition of hydrogen sulfide and its genesis in Sichuan basin,” *Geochimica*, vol. 35, pp. 333–345, 2006.
- [12] Q. Y. Liu, R. H. Worden, Z. J. Jin et al., “TSR versus non-TSR processes and their impact on gas geochemistry and carbon stable isotopes in Carboniferous, Permian and Lower Triassic marine carbonate gas reservoirs in the Eastern Sichuan Basin, China,” *Geochimica et Cosmochimica Acta*, vol. 100, pp. 96–115, 2013.
- [13] C. Cai, L. Xiang, Y. Yuan et al., “Sulfur and carbon isotopic compositions of the Permian to Triassic TSR and non-TSR altered solid bitumen and its parent source rock in NE Sichuan Basin,” *Organic Geochemistry*, vol. 105, pp. 1–12, 2017.
- [14] G. Y. Zhu, A. G. Fei, J. Zhao, and C. Liu, “Sulfur isotopic fractionation and mechanism for thermochemical sulfate reduction genetic H<sub>2</sub>S,” *Acta Petrologica Sinica*, vol. 30, no. 12, pp. 3772–3786, 2014.
- [15] R. H. Worden, P. C. Smalley, and N. H. Oxtoby, “Gas souring by thermochemical sulfate reduction at 140°C,” *AAPG Bulletin*, vol. 79, pp. 854–863, 1995.
- [16] M. M. Cross, D. A. C. Manning, S. H. Bottrell, and R. H. Worden, “Thermochemical sulphate reduction (TSR): experimental determination of reaction kinetics and implications of the observed reaction rates for petroleum reservoirs,” *Organic Geochemistry*, vol. 35, no. 4, pp. 393–404, 2004.
- [17] F. Hao, T. Guo, Y. Zhu, X. Cai, H. Zou, and P. Li, “Evidence for multiple stages of oil cracking and thermochemical sulfate reduction in the Puguang gas field, Sichuan Basin, China,” *AAPG Bulletin*, vol. 92, no. 5, pp. 611–637, 2008.
- [18] Q. Ma, G. S. Ellis, A. Amrani, T. Zhang, and Y. Tang, “Theoretical study on the reactivity of sulfate species with hydrocarbons,” *Geochimica et Cosmochimica Acta*, vol. 72, no. 18, pp. 4565–4576, 2008.
- [19] T. Zhang, G. S. Ellis, Q. Ma, A. Amrani, and Y. Tang, “Kinetics of uncatalyzed thermochemical sulfate reduction by sulfur-free paraffin,” *Geochimica et Cosmochimica Acta*, vol. 96, pp. 1–17, 2012.
- [20] T. G. Powell and R. W. Macqueen, “Precipitation of sulfide ores and organic matter: sulfate reactions at Pine Point, Canada,” *Science*, vol. 224, no. 4644, pp. 63–66, 1984.
- [21] J. S. Seewald, “Organic-inorganic interactions in petroleum producing sedimentary basins,” *Nature*, vol. 426, no. 6964, pp. 327–333, 2003.
- [22] L. Jiang, R. H. Worden, and C. Cai, “Generation of isotopically and compositionally distinct water during thermochemical sulfate reduction (TSR) in carbonate reservoirs: Triassic Feixianguan Formation, Sichuan Basin, China,” *Geochimica et Cosmochimica Acta*, vol. 165, pp. 249–262, 2015.
- [23] C. N. Zou, L. H. Hou, S. Z. Tao et al., “Hydrocarbon accumulation mechanism and structure of large-scale volcanic weathering crust of the Carboniferous in northern Xinjiang, China,” *Science China Earth Sciences*, vol. 55, no. 2, pp. 221–235, 2012.
- [24] D. Song, D. He, and S. Wang, “Source rock potential and organic geochemistry of Carboniferous source rocks in Santanghu Basin, NW China,” *Journal of Earth Science*, vol. 24, no. 3, pp. 355–370, 2013.
- [25] W. Li, Y. Q. Liu, Y. P. Dong et al., “The geochemical characteristics, geochronology and tectonic significance of the Carboniferous volcanic rocks of the Santanghu area in northeastern Xinjiang, China,” *Science China Earth Sciences*, vol. 56, no. 8, pp. 1318–1333, 2013.
- [26] W. M. Li and R. Y. Zhang, “Reservoir characteristics of composite petroleum system in Santanghu basin,” *Xinjiang Petroleum Geology*, vol. 21, pp. 275–278, 2000.
- [27] H. Jian-rong, L. Yi-qun, F. Qiao, X. Xiu-juan, and Z. Xiao-qin, “The tectonic-thermal evolution of the Santanghu Basin,” *Journal of Northwest University (Natural Science Edition)*, vol. 36, pp. 290–294, 2006.
- [28] L. Jun, B. Liang-Man, L. Wei et al., “Size distribution of sulfur species in fine and ultrafine aerosol particles using sulfur K-

- edge XANES,” *Chinese Physics C*, vol. 33, no. 11, pp. 965–968, 2009.
- [29] S. Xinhua, B. Guojuan, C. Changxu, C. Xiaoying, and W. Binwen, “Study on waterflooding feasibility of volcanic reservoir in Niudong,” *Tuha Oil & Gas*, vol. 15, pp. 262–266, 2010.
- [30] T. Zhang, G. S. Ellis, K.-s. Wang et al., “Effect of hydrocarbon type on thermochemical sulfate reduction,” *Organic Geochemistry*, vol. 38, no. 6, pp. 897–910, 2007.
- [31] K.-l. DING, S.-y. LI, C.-t. YUE, and N.-n. ZHONG, “Simulation experiments on thermochemical sulfate reduction using natural gas,” *Journal of Fuel Chemistry and Technology*, vol. 35, no. 4, pp. 401–406, 2007.
- [32] H. Li, C. Cai, L. Jia, C. Xu, and K. Zhang, “The effect of water chemistry on thermochemical sulfate reduction: a case study from the Ordovician in the Tazhong area, Northwest China,” *Geofluids*, vol. 2017, Article ID 6351382, 11 pages, 2017.
- [33] C. Cai, G. Hu, H. X. Li et al., “Origins and fates of H<sub>2</sub>S in the Cambrian and Ordovician in Tazhong area: evidence from sulfur isotopes, fluid inclusions and production data,” *Marine and Petroleum Geology*, vol. 67, pp. 408–418, 2015.
- [34] H. P. Taylor Jr, J. Frechen, and E. T. Degens, “Oxygen and carbon isotope studies of carbonatites from the Laacher See District, West Germany and the Alnö District, Sweden,” *Geochimica et Cosmochimica Acta*, vol. 31, no. 3, pp. 407–430, 1967.
- [35] Y. Nan, Y. Q. Liu, D. W. Zhou, N. C. Zhou, X. Jiao, and P. Zhou, “Characteristics and origin of amygdale and crack fillers in volcanic rock of Late Carboniferous in Santanghu basin, Xinjiang,” *Acta Petrologica Sinica*, vol. 32, pp. 1901–1913, 2016.



**Hindawi**

Submit your manuscripts at  
[www.hindawi.com](http://www.hindawi.com)

